

Histone H1⁰ and Its Carboxyl-Terminal Domain Bind in the Major Groove of DNA[†]

Naila M. Mamoon, Yuguang Song, and Susan E. Wellman*

*Department of Pharmacology and Toxicology, University of Mississippi Medical Center,
2500 North State Street, Jackson, Mississippi 39216-4505**Received March 12, 2002; Revised Manuscript Received May 30, 2002*

ABSTRACT: The binding of histone H1⁰ to T4 bacteriophage DNA was investigated using thermal denaturation of the DNA titrated with varying concentrations of protein. The H1⁰ used was expressed in and purified from a strain of *E. coli* and is therefore homogeneous with respect to H1 subtype and posttranslational modifications. Two types of T4 DNA were used: wild-type, which contains a modification of the cytosine residues that projects into the major groove: and a mutant type, which lacks the modification of the cytosines. Data were compared to simulated thermal denaturation curves to determine estimates for binding affinity and binding site size in base pairs of the protein. Analysis of the data yielded values of 10^8 M^{-1} for K , the binding affinity, and 10 base pairs for n , the number of base pairs covered by one protein, for the mutant T4 DNA. Analysis of the wild-type DNA data suggested that the glucose projecting into the major groove of this DNA decreases the number of sites to which the H1⁰ protein can bind, indicating that there are interactions between the protein and the major groove of DNA. The binding site size on this DNA is 10 base pairs, the same as on the unmodified DNA. The affinity for wild-type DNA is slightly higher, 10^9 M^{-1} . Data were collected and analyzed for binding of two domains of the protein as well, the carboxyl-terminal domain and the central globular domain. Binding of the carboxyl-terminal domain was quantitatively and qualitatively similar to that of the full-length protein. In contrast, binding of the globular domain was quite different: it binds much more weakly, with a K of $6 \times 10^4 \text{ M}^{-1}$, and covers fewer base pairs, with an n of 3. Also, there was no evidence that the globular domain interacts with the major groove of DNA.

DNA in the eukaryotic cell is compacted and organized into chromatin. The proteins that are primarily responsible for folding DNA into chromatin are the histones, small basic proteins. The core histones, with DNA, form the nucleosomal core particle. Further folding, beyond that facilitated by the core histones, is mediated by the linker, or H1, histones (reviewed in 1–5).

H1 histones bind not only to nucleosomal DNA but also to free DNA, and our focus has been the elucidation of the intrinsic DNA binding properties of the H1 histones. A model that accurately describes binding of H1 histone to DNA has been elusive. Binding is quite complex, with evidence for positive cooperativity (5–11) and for conformational changes in the DNA and protein (12–19). Binding of H1 histone to DNA ultimately leads to condensation of the DNA, and it is not known whether this reflects only conformational changes in the DNA or whether protein–protein interactions are also involved. [In fact, it has been suggested that H1 histones have DNA binding sites on at least two surfaces of the proteins, and that they would therefore cross-link strands of DNA (reviewed in 2); clearly, however, in the presence of DNA rather than of nucleosomes, intramolecular folding or bending of DNA would be at least as likely.] Complicating the investigations are technical problems: for one, typical

approaches to quantitatively measure binding require separation of the unbound protein from the protein complex, which is difficult in the case of H1 histone and H1–DNA complexes; in addition, binding affinity appears to be sufficiently great that at low levels of saturation of the DNA, the concentration of unbound ligand is too small to be accurately measured.

The approach that we have taken to obviate these technical problems is that of measuring thermal denaturation of DNA in the presence of varying concentrations of H1 proteins. By means of this approach, using the procedures described by McGhee (20), we are able to determine quantitative parameters of binding, including intrinsic affinities, number of base pairs covered by one protein, and values for cooperativity parameters. We use the model of McGhee and von Hippel (21), which describes the binding of nonspecific ligands to DNA.

How does histone H1 interact with DNA? The protein could bind in the major or minor groove of DNA, to the DNA phosphates, or to any combination of these structures. The question of whether H1 histones bind in the major groove or in the minor groove or both has implications for their binding to nucleosomes. The exact mode of interaction of the H1 histones with the nucleosome is not known. There are currently several models that are debated. In the model proposed by Crane-Robinson and Ptitsyn (22), the linker histone is envisaged as binding symmetrically to the nucleosome where three strands of DNA meet, at the entry/exit point of the nucleosome: where the DNA strand enters, is

[†] This work was supported by Grant R06/CCR419466 from the Centers for Disease Control.

* To whom correspondence should be addressed. Telephone: 601 984 1631. E-mail: swellman@pharmacology.umsmed.edu.

wrapped around, and exits the nucleosome. One consequence of this model is that the H1 histone would be positioned such that the globular domain of the protein interacts with the minor groove of the DNA. An alternative model proposes asymmetric binding at the nucleosome entry/exit point, with the H1 histone lying "inside" the DNA gyre and to one side of the nucleosome (23–25). In this model, the major groove of the DNA would be positioned to interact with the H1 histone.

We have used the genomic DNA of T4 bacteriophage to investigate the binding of one H1 histone subtype, H1⁰, in the major groove of DNA. The DNA of the wild-type bacteriophage has glucose covalently attached to cytosines (26). The glucose moiety projects into the major groove, resulting in a partial block of the major groove. This modification does not perturb the helix, but does interfere with binding of drugs in the major groove (27). As a control, we have used DNA from a mutant strain that lacks the enzyme systems for modifying its DNA (28). DNA from the mutant strain is identical (except for the mutations that knock out the modification system) to that of the wild-type strain, except that the major groove is not glucosylated.

In addition to investigating binding of the whole H1⁰ protein, we investigated the binding of two individual domains: the globular domain and the carboxyl-terminal domain. The globular domain consists of amino acids 22–84. The globular domain is the only portion of the protein that is folded in solution (29–31) and is the only portion of the protein that has been crystallized (32). The carboxyl-terminal domain consists of the 110 carboxyl-terminal amino acids. It is very lysine rich, and does not fold in solution, presumably because of electrostatic repulsion between the lysine residues. Earlier studies have been carried out with domains of the H1 histones (see Discussion), but these studies primarily used protein fragments that would be heterogeneous; the domain peptides were generated by proteolysis of the H1 fraction, and the H1 fraction typically would include at least several different subtypes of H1 histone (33). In contrast, our studies have used proteins made by recombinant techniques, purified by HPLC, and identified using mass spectrometry, ensuring that the proteins are homogeneous.

EXPERIMENTAL PROCEDURES

Proteins. H1⁰. Construction of the bacterial strain that expresses histone H1⁰ and expression and purification of the protein have been described (34).

Carboxyl-Terminal Domain. The plasmid for expression of the carboxyl-terminal domain of H1⁰ (H1⁰-C) was constructed from the expression clone containing the full-length gene, using the QuickChange site-directed mutagenesis kit (Stratagene) to introduce an *Nco*I site at the start of the C-terminal domain. The sequence ³¹⁴CGGTGGCT... was changed to ³¹⁴CCATGGCT.... The corresponding protein sequence is MAFKKEV..., with the K indicated in boldface type corresponding to K₁₀₇ of the full-length protein, the approximate start of the C-terminal domain (35, 36). The plasmid was digested with *Nco*I, religated, and used to transform *E. coli* strain BL21(DE3)pLysS (Novagen). Expression and purification of H1⁰-C was identical to that of

H1⁰ (34), up to the step of perchloric acid extraction. The supernatant from the perchloric acid extraction was not precipitated with acetone, but was directly injected onto the reverse-phase HPLC column, from which it eluted at approximately 15 min. The entire peak was collected and run on an HPLC ion-exchange column, as described (34). The back half of a peak eluting at approximately 23 min was collected and determined to be pure H1⁰-C. Mass spectrometry indicated that the molecular weight of the expressed protein is 9544. This is in agreement with the predicted molecular weight without the N-terminal methionine, 9546.

Globular Domain. The gene coding for the globular domain (H1⁰-G), amino acids T₂₂–F₁₀₆, was made by amplifying the corresponding region of the full-length H1⁰ gene. The primers used were 5'-GACCATGGCTACGGAC-CACCCCAA and 5'-TAGGATCCTCAGAAAGCCAC-CGACC. Use of these primers resulted in incorporation of an *Nco*I site and an additional A codon at the 5'-end of the gene, and a stop codon and *Bam*HI site at the 3'-end of the gene. Construction of the plasmid and transformation of BL21(DE3)pLysS were as described (34). Growth of the bacterial cells and induction of expression were as described (34). Washed, pelleted cells were frozen and then resuspended in buffer consisting of 50 mM Tris-HCl, 50 mM EDTA, pH 8.0. Cells from 50 mL of culture, resuspended in 2 mL of buffer, were processed at a time. The resuspended cells were sonicated for 9–10 min, using a Fisher model 60 Sonic Dismembrator. At the power setting used, the output was approximately 4 W. Cells were kept on ice during sonication. After 30 min on ice, the sonicated cells were centrifuged at 31000g for 20 min at 4 °C. The supernatant was adjusted to 5% perchloric acid and incubated on ice for 45 min. The extract was centrifuged at 31000g for 30 min at 4 °C. The supernatant was collected for injection onto the reverse-phase HPLC column. The column and buffers have been described (34). The gradient used was 5.3–30.3% Buffer B in 10 min, 30.3–41.6% Buffer B in 15 min, and 41.6–46.1% Buffer B in 9 min. H1⁰-G eluted at about 27 min. Mass spectrometry showed the molecular weight of the expressed protein to be 9348, which is that predicted for the peptide without the N-terminal methionine.

Protein concentration was determined from the A₂₀₅ of solutions of proteins in water, using extinction coefficients of 27.8, 31.1, and 28.6 mL mg⁻¹ cm⁻¹ for H1⁰, H1⁰-C, and H1⁰-G, respectively, determined as described (37).

DNA. Wild-type T4 bacteriophage was grown in *E. coli* strain K704. The mutant T4 bacteriophage, T4Cyt, defective in genes *denA*, *denB*, *gene56*, and *alc*, was a kind gift from Dr. Larry Snyder. The primary lysate of T4Cyt was grown in *E. coli* strain K803. The secondary lysate was grown in the permissive *E. coli* host B834 *galU56* in one infective cycle (38). Phage particles were purified using precipitation with poly(ethylene glycol) and NaCl, followed by sedimentation in cesium chloride, as described (39). Purification of phage DNA was as described (39). The concentration of DNA was calculated from molar extinction coefficients of 12 663 M⁻¹ bp cm⁻¹ for wild-type and 12 752 M⁻¹ bp cm⁻¹ for T4Cyt, determined as described (40). Both types of DNA were treated with the restriction endonuclease *Eco*RI; the susceptibility of T4Cyt DNA to digestion confirmed the absence of modified cytosines in the DNA, and the resistance

of T4 wild-type DNA confirmed their presence in this DNA (data not shown).

Binding Reactions. Solutions of DNA and protein in phosphate buffer (6 mM Na₂HPO₄, 2 mM NaH₂PO₄, pH 7.3) were mixed and allowed to set at room temperature for 1 h before thermal denaturation was initiated [binding of H1 histone to chromatin appears to be at equilibrium within 30 min (41); we have seen no difference in thermal denaturation curves for H1⁰-DNA solutions incubated for 1 h or for up to 24 h (data not shown).]

Thermal Denaturation. Thermal denaturation was monitored at 260 nm in a Cary 100 spectrophotometer. Temperature was increased 1 °C per minute. The absorbance data were converted to fraction coil as described (42 and reference 30 cited within).

Simulations. The simulated thermal denaturation curves were calculated as described (42, 43) using a computer program written by McGhee (20) that is based on the McGhee–von Hippel model for DNA–ligand interactions (21). The DNA parameters needed for the calculations were DNA concentration (in mole base pairs), T_M , the temperature at the midpoint of the DNA helix–coil transition (determined from the DNA-only curve), the enthalpy of the helix–coil transition, and σ , which was determined empirically from simulations of the DNA-only transition to be 5×10^{-4} . The enthalpy of the helix–coil transition for the T4 DNA was determined using differential scanning calorimetry (data not shown) and is $7634 \text{ cal mol}^{-1} \text{ K}^{-1}$. The protein parameters used in the calculations were K , binding affinity expressed in units of M^{-1} , n , number of base pairs covered by one bound protein, and protein concentration. We used a value of zero for binding affinity for single-stranded DNA (see 42 for discussion) and for ΔH of binding to double-stranded DNA (42, 44). As we have pointed out previously (42), because these curves are simulations and not fitted curves, we have no estimate of the errors in the parameters. However, the simulations can be quite sensitive to small changes in parameters, and so in practice the range of values that in combination will reproduce the experimental data is very small (42, 43). For the simulations presented here, increasing or decreasing n by 1 or K by a factor of 2 produced curves that clearly did not match the experimental data as well.

RESULTS

In Figure 1 are shown the thermal denaturation curves of T4Cyt DNA titrated with H1⁰. At the lowest concentration of H1⁰ used, the curve shifts to the right and begins to broaden, indicating that the protein binds to the double-stranded DNA (either exclusively or with much higher affinity than to the single-stranded DNA; see 20, and 42 for discussion). As protein concentration is increased, the thermal denaturation curves become biphasic, as predicted by McGhee (20). For T4Cyt DNA, which is unmodified in its major groove, the simulated curves that closely approximate the experimental data were calculated using K , the affinity constant, equal to 10^8 M^{-1} and n , the number of base pairs bound per protein, of 10 (Table 1). We also observed no evidence for positive cooperativity (see Discussion).

In Figure 2 are shown thermal denaturation curves of T4 wild-type DNA, which is modified in its major groove, titrated with H1⁰. Our initial hypothesis was that H1⁰ does

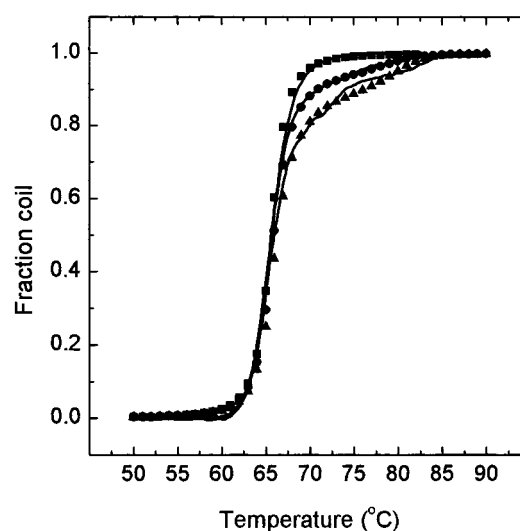


FIGURE 1: T4Cyt DNA titrated with H1⁰. The concentration of DNA was $36 \mu\text{M}$ base pairs. The solid lines are experimental data for DNA only, DNA in the presence of 150 nM H1⁰, and DNA in the presence of 300 nM H1⁰. The symbols indicate curves that were simulated using a K of 10^8 M^{-1} and an n of 10 base pairs.

Table 1: Parameters Used for Simulating the Thermal Denaturation Curves Shown

	T4Cyt		T4 wild-type		$^a[\text{DNA}]_{\text{app}} (\mu\text{M})$
	n (bp)	$K (\text{M}^{-1})$	n (bp)	$K (\text{M}^{-1})$	
H1 ⁰	10	1×10^8	10	1×10^9	13^b
H1 ⁰ -C	10	5×10^8	10	2×10^9	15^b
H1 ⁰ -G	3	6×10^4	3	6×10^4	33^c

^a DNA concentration used in the simulation. ^b Actual DNA concentration was $33.9 \mu\text{M}$ base pairs. ^c Actual DNA concentration was the same as apparent.

not bind in the major groove of DNA, and that therefore binding of H1⁰ to DNA that is modified in its major groove would be the same as to the identical DNA sequence that is unmodified. Differences from the results with T4Cyt DNA are obvious from inspection; at the same concentrations of H1, thermal denaturation curves of the wild-type DNA are shifted more dramatically than are the curves of the T4Cyt. This difference immediately answers the question of whether H1⁰ interacts in the major groove of DNA. The answer is that it must; since the sequences of T4Cyt and T4 wild-type are nearly identical, there should otherwise be no difference between the results for the two different types of DNA. We considered several possibilities for the differences in binding to modified versus unmodified DNA: that the glucose projecting into the major groove affected n , the number of base pairs bound by the protein (either increasing or decreasing the site size), that K , the affinity of the protein for the DNA, was altered (either increased or decreased), or that both n and K were altered, in any combination. We also considered the possibility that the modified bases were simply not available for binding, and that the concentration of sites was less than that of the comparable concentration of unmodified DNA. After calculating curves for all of these possibilities and comparing the calculated curves to experimental curves, we concluded that the latter explanation, that the modified bases were not available for binding, is most likely to be correct. We were unable to obtain satisfactory simulations (data not shown) unless we assumed that the

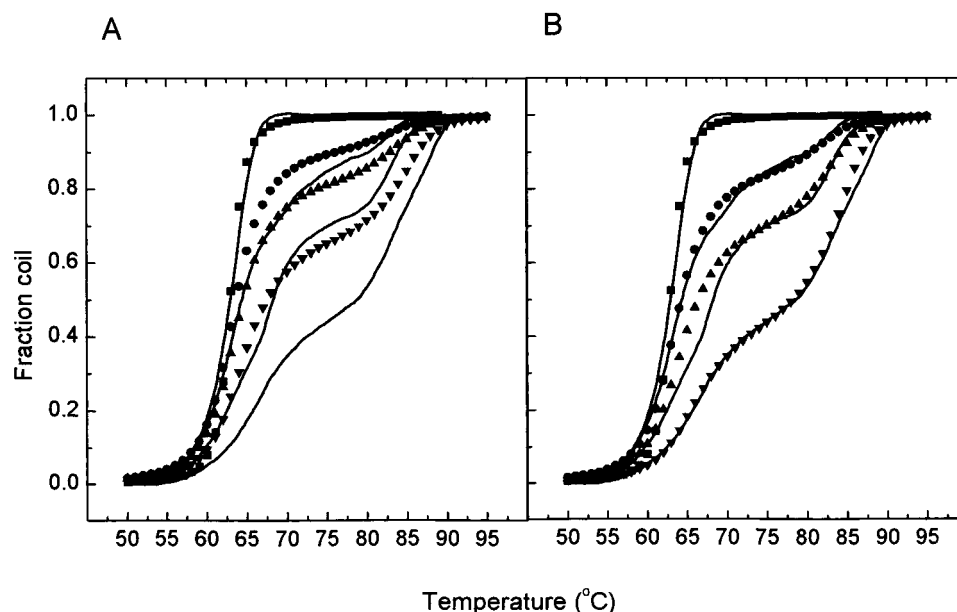


FIGURE 2: T4 wild-type DNA titrated with H1⁰. The concentration of DNA was 33.9 μM base pairs. The solid lines are experimental data for DNA only, DNA in the presence of 150 nM H1⁰, DNA in the presence of 300 nM H1⁰, and DNA in the presence of 600 nM H1⁰. The symbols indicate curves that were simulated using a K of 10^9 M^{-1} and an n of 10 base pairs. (A) DNA concentration used in the simulations was 22 μM base pairs. (B) DNA concentration used in the simulations was 13 μM base pairs.

modified bases result in a decrease in the number of sites available to H1⁰. The calculated curves shown in Figure 2 are calculated using K equal to 10^9 M^{-1} and an n of 10 base pairs, similar to the parameters used to calculate curves for cytosine DNA. In Figure 2A, the DNA concentration used in the calculations was 22 μM base pairs, which corresponds to the concentration of unmodified base pairs. Because the H1⁰ binds to more than one base pair, modification of the cytosines, about 34% of the bases in the wild-type DNA, is likely to eliminate more than 34% of the binding sites. In Figure 2B are shown curves calculated with the same ligand parameters, but with a DNA concentration of 13 μM base pairs (Table 1). These calculated curves are nearly identical to the experimental curves.

Analysis of the data for the carboxyl-terminal domain of H1⁰, H1⁰-C, yielded similar results, indicating that the interaction of the carboxyl-terminal domain with DNA is similar to that of the full-length protein. In Figure 3 are shown experimental and calculated thermal denaturation curves for T4Cyt DNA titrated with H1⁰-C. The simulated curves were calculated using a K of $5 \times 10^8 \text{ M}^{-1}$ and an n of 10 base pairs (Table 1). For the T4 wild-type DNA data, shown in Figure 4, it was necessary to assume modified bases were unavailable for binding and therefore to use a decreased DNA concentration in the calculated curves. The parameters used in the calculations were a K of $2 \times 10^9 \text{ M}^{-1}$, an n of 10 base pairs, and a DNA concentration of 15 μM base pairs (Table 1).

H1⁰-G, the globular domain of H1⁰, appears to bind far more weakly to bulk DNA than either the full-length or the carboxyl-terminal domain. Thermal denaturation curves of DNA titrated with H1⁰-G are shown in Figures 5 and 6. Much higher concentrations were required to shift the thermal denaturation curves at all, approximately 1 μM versus around 100 nM for H1⁰-C and the full-size H1⁰. For T4Cyt DNA, shown in Figure 5, the parameters used in the simulated curves were a K of $6 \times 10^4 \text{ M}^{-1}$ and an n of 3 base pairs

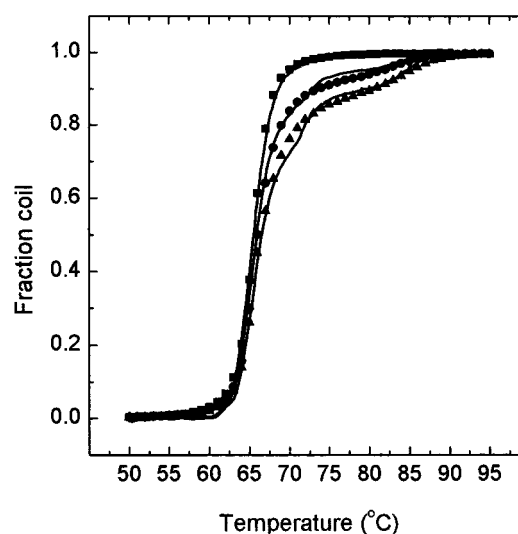


FIGURE 3: T4Cyt DNA titrated with H1⁰-C. The concentration of DNA was 29.3 μM base pairs. The solid lines are experimental data for DNA only, DNA in the presence of 150 nM H1⁰-C, and DNA in the presence of 250 nM H1⁰-C. The symbols indicate curves that were simulated using a K of $5 \times 10^8 \text{ M}^{-1}$ and an n of 10 base pairs.

(Table 1). The binding of H1⁰-G to T4 wild-type DNA appeared insensitive to the modification of the major groove: the simulated curves in Figure 6 were calculated using the same parameters as for T4Cyt DNA, a K of $6 \times 10^4 \text{ M}^{-1}$ and an n of 3 base pairs (Table 1). No adjustment to DNA concentration was necessary.

DISCUSSION

The binding of H1 to DNA is complex and is not well understood; because of the technical difficulties associated with rigorous methods for directly determining binding parameters, few attempts have been made to collect and analyze data that yield precise, quantitative information on binding. One of the only truly quantitative studies of binding

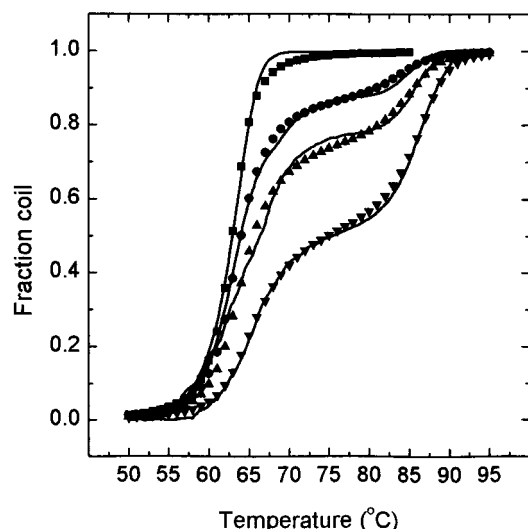


FIGURE 4: T4 wild-type DNA titrated with $H1^0$ -C. The concentration of DNA was $33.9 \mu\text{M}$ base pairs. The solid lines are experimental data for DNA only, DNA in the presence of 150 nM $H1^0$ -C, DNA in the presence of 300 nM $H1^0$ -C, and DNA in the presence of 600 nM $H1^0$ -C. The symbols indicate curves that were simulated using a K of $2 \times 10^9 \text{ M}^{-1}$ and an n of 10 base pairs. DNA concentration used in the simulations was $15 \mu\text{M}$ base pairs.

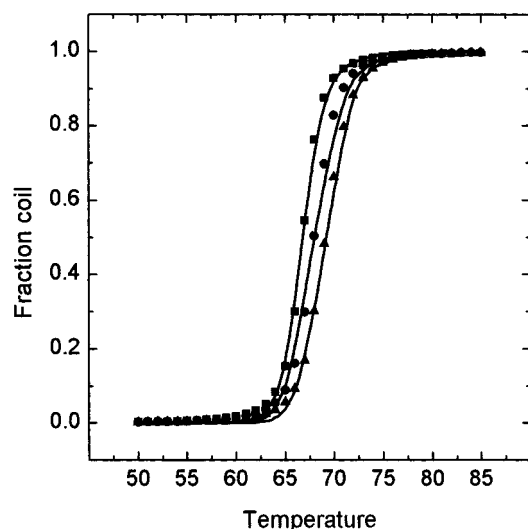


FIGURE 5: T4Cyt DNA titrated with $H1^0$ -G. The concentration of DNA was $29.3 \mu\text{M}$ base pairs. The solid lines are experimental data for DNA only, DNA in the presence of $1.2 \mu\text{M}$ $H1^0$ -G, and DNA in the presence of $2.4 \mu\text{M}$ $H1^0$ -G. The symbols indicate curves that were simulated using a K of $6 \times 10^4 \text{ M}^{-1}$ and an n of 3 base pairs.

of H1 was that of Watanabe (7). Using fluorescently labeled H1 histone, Watanabe determined a binding affinity of $3.6 \times 10^7 \text{ M}^{-1}$ of calf histone H1 for calf thymus DNA (in 0.2 M NaCl). He also observed no cooperativity of binding at NaCl concentrations below about 20 mM . There is a significant difference between the materials that he used and those used by us; at the time of those studies, recombinant histone H1 was not available, and thus the protein used by him was a mixture of H1 variant types, as well as possibly including a small amount of non-histone protein. In addition, the protein that was used was modified by addition of fluorescein moieties to at least a few of the lysines, which would likely affect the interactions. Nevertheless, the results of our studies with T4Cyt DNA are in reasonable agreement

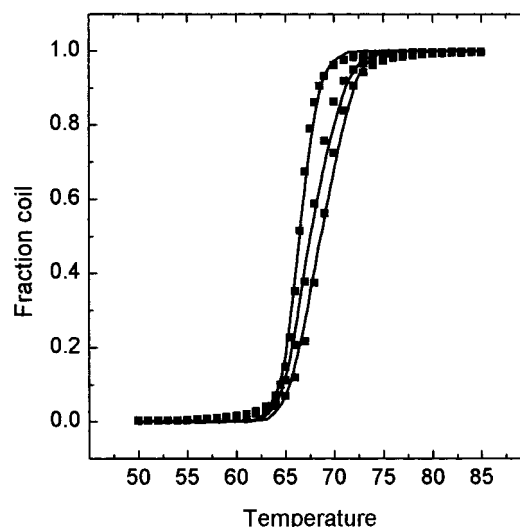


FIGURE 6: T4 wild-type DNA titrated with $H1^0$ -G. The concentration of DNA was $31.8 \mu\text{M}$ base pairs. All other details are the same as for Figure 5.

with his, with affinity constants of 10^8 – 10^9 M^{-1} (slightly higher than his determinations, as expected at the lower salt concentration that we used), and no apparent positive cooperativity (see below). The other quantitative data available are from our own lab (42). We had used the method of thermal denaturation and simulation of curves to investigate binding of $H1^0$ to homopolymers. Our results suggested higher affinities, in the range of 10^{10} – 10^{15} M^{-1} . However, as acknowledged within the publication, the simulated curves did not satisfactorily reflect the data. We had discussed several possible reasons for the unsatisfactory simulations (42). Perhaps the homopolymers have different structural properties, arising from the repeating dinucleotides, than do the natural DNA molecules, which influence the binding of $H1^0$.

Our results show that binding of $H1^0$ is affected by a modification that projects into the major groove. Theoretically, effects other than direct effects on binding could result in changes in the thermal denaturation curves. However, the analysis of our data suggests that the modification of the major groove reduces the concentration of binding sites, which indicates that the protein directly interacts in the major groove. Binding of H1 histones is relatively non-sequence-specific; instead, it is thought that H1 is selective for sequence-dependent conformations. Because sequence-specific recognition is usually thought to require base-specific interactions in the major groove, and because H1 histones do not bind preferentially to a specific sequence, interactions of H1 histones in the major groove of DNA have been considered to be relatively minor. Also, characteristics of the interactions are consistent with binding in the minor groove; e.g., the binding is largely electrostatic, and electrostatic interactions have been suggested to be consistent with binding in the minor groove to AT base pairs, which have higher electrostatic potential in the minor groove (45, 46). The work of Laemmli's lab has suggested preferential binding to AT-rich DNA (47), and has shown that distamycin, a drug that binds in the minor groove, competes with H1 histone for binding to DNA (48). Recently, however, attention has focused on the possibility of major groove interactions, with the determination of the crystal structure

of the globular domain, which is similar to that of catabolite activator protein (CAP) and to hepatocyte nuclear transcription factor (HNF) (32), transcriptional factors that bind in the major groove of DNA.

The carboxyl-terminal domain, too, interacts with the major groove. The carboxyl-terminal domain binds with similar, if not slightly higher, affinity, and to same number of base pairs, as does the intact protein, consistent with earlier inferences that most binding activity resides in this domain: Bradbury et al. (30) showed that the amino-terminal 106 amino acids of calf thymus H1 bound only weakly to DNA, and that the carboxyl-terminal portion bound as tightly as did the entire protein. Consistent with the idea that the DNA binding activity resides in the carboxyl-terminal domain, Morán et al. (16) showed that the ability of H1 to change DNA structure from B-DNA to Ψ -DNA is a property of the carboxyl-terminal domain.

In contrast, binding of the globular domain did not appear to be affected by the modification projecting into the major groove. It has been proposed that the globular domain interacts with the major groove of DNA, because of the similarities between its structure and those of HNF and CAP (32), but there was no apparent effect on binding of having the modification of the major groove. The obvious possible explanation is that the globular domain simply does not bind in the major groove. In fact, binding of the globular domain, to bulk DNA at least, is quite weak, and few base pairs are covered. This is consistent with earlier results that suggested little importance of the globular domain in binding of DNA, e.g., the results of Bradbury et al. (44), as well as those of Morán et al. (16). We cannot, however, eliminate the possibility that the globular domain interacts more strongly with a specific sequence or specific sequences, like the transcription factors that it is said to resemble. Sequence-specificity could also account for the absence of differences between binding to T4 wild-type and T4Cyt DNA; if the globular domain binds preferentially to a specific sequence, and if this sequence does not include cytosine, which was the only type of residue modified, then no difference would be observed in binding of the globular domain to the two types of DNA.

These results do not, of course, exclude the possibility that the full-length protein and the carboxyl-terminal domain also bind in the minor groove. We were unable to address the question of minor groove interactions with this experimental approach.

A range of values for number of base pairs bound per H1 has been reported; Watanabe (7) calculated a value of 65 bases (not base pairs) for the binding site, and others have reported values of 15–80 base pairs (49, 50). When we added H1⁰ to DNA at a ratio of about 1 protein to 30 base pairs, the solution become turbid, which reflects a conformational change in the DNA, described by many others (12, 14, 16–18). Because most others who have investigated binding of H1 have monitored the phenomenon of conformational change, an indirect measure of binding, they concluded that the DNA was saturated at this binding ratio. We observe, however, in our binding studies in which we measure free protein concentration, that additional H1⁰ can bind, and saturation occurs at approximately 1 protein per 10 base pairs (data not shown). From our data with homocopolymers (42), we had derived values of 20–30 base

pairs for H1⁰. However, we also determined much higher values of K (see above), and n and K are correlated in the McGhee–von Hippel model (21). The simulated curves for the homocopolymers did not agree nearly as well with the data as do the simulated curves presented for binding to the T4 DNA species, which show excellent agreement with the experimental data. For this reason, we believe that the n and K values we calculated for binding of H1⁰ to the homocopolymers are less likely to be the true values than those values calculated for the natural DNA species.

We obtained very close approximations of the experimental data without including a cooperativity parameter in the simulations. While H1 histone has been reported to bind to DNA with positive cooperativity, most reports suggest that binding is cooperative only if the NaCl concentration is greater than about 20 mM (7, 8), and we performed our experiments in 15 mM buffer. Another consideration is that, as discussed by Kowalczykowski et al. (51), at binding densities that are less than 0.1 divided by ω , the amount of ligand bound to the DNA lattice is independent of ω . In the case of H1⁰, we have data consistent with an ω of 10 (data not shown); 0.1 divided by an ω of 10 would equal 0.01. Under the experimental conditions that we used, the binding densities did not exceed this value: DNA concentrations were approximately 30 μ M base pairs, and TOTAL protein concentrations did not exceed 300 nM. We confirmed that data simulated with a K of 10^8 M⁻¹ and an n of 10 were relatively insensitive to an ω of 10 (data not shown).

CONCLUSIONS

The use of DNA from the two different T4 bacteriophages has allowed us to unambiguously determine that there are interactions between H1⁰ and the major groove of DNA. Use of the unmodified DNA has yielded quantitative answers as well: estimates for the binding affinity of 10^8 M⁻¹ and for the binding site size of 10 base pairs. The proposed dominance of the carboxyl-terminal domain in the binding interaction has been confirmed, and it is clear that the globular domain binds weakly to bulk DNA. What is not known from these studies is if there are interactions in the minor groove as well. Also unanswered is if the globular domain binds to a specific DNA sequence or sequences with high affinity, a property that would be masked by the use of bulk DNA.

ACKNOWLEDGMENT

We thank Drs. Abulhair Mamoon and Don Sittman for helpful suggestions on the manuscript.

REFERENCES

1. van Holde, K. E. (1989) *Chromatin*, Springer-Verlag, New York.
2. Ramakrishnan, V. (1997) *Annu. Rev. Biophys. Biomol. Struct.* 26, 83–112.
3. Bradbury, E. M. (1998) *J. Cell. Biochem., Suppl.* 30–31, 177–184.
4. Thomas, J. O. (1999) *Curr. Opin. Cell Biol.* 11, 312–317.
5. Hayes, J. J., and Hansen, J. C. (2001) *Curr. Opin. Genet. Dev.* 11, 124–129.
6. Renz, M., and Day, L. A. (1976) *Biochemistry* 15, 3220–3227.
7. Watanabe, F. (1986) *Nucleic Acids Res.* 14, 3573–3586.
8. Clark, D. J., and Thomas, J. O. (1986) *J. Mol. Biol.* 187, 569–580.
9. Rodríguez, A. T., Perez, L., Morán, F., Montero, F., and Suau, P. (1991) *Biophys. Chem.* 39, 145–152.

10. Thomas, J. O., Rees, C., and Finch, J. T. (1992) *Nucleic Acids Res.* 20, 187–194.
11. Wellman, S. E., Sittman, D. B., and Chaires, J. B. (1994) *Biochemistry* 33, 384–388.
12. Hsiang, M. W., and Cole, R. D. (1977) *Proc. Natl. Acad. Sci. U.S.A.* 74, 4852–4856.
13. Palau, J., Climent, F., Aviles, F. J., Morros, A., and Soliva, M. (1977) *Biophys. Acta* 476, 108–121.
14. Thoma, F., and Koller, T. (1977) *Cell* 12, 101–107.
15. Aviles, F. J., Diez-Cabellero, T., Palau, J., and Albert, A. (1978) *Biochimie* 4, 445–451.
16. Morán, F., Montero, F., Azorín, F., and Suau, P. (1985) *Biophys. Chem.* 22, 125–129.
17. Girardet, J. L., Casas, M. T., Cornudella, L., Gorka, C., Lawrence, J. J., and Mura, C. V. (1988) *Biophys. Chem.* 31, 275–286.
18. Yao, J., Lowary, P. T., and Widom, J. (1991) *Biochemistry* 30, 8408–8414.
19. Vila, R., Ponte, I., Collado, M., Arrondo, J. L., Jimenez, M. A., Rico, M., and Suau, P. (2001) *J. Biol. Chem.* 276, 46429–46435.
20. McGhee, J. D. (1976) *Biopolymers* 15, 1345–1375.
21. McGhee, J. D., and von Hippel, P. H. (1974) *J. Mol. Biol.* 86, 469–489.
22. Crane-Robinson, C., and Ptitsyn, O. B. (1989) *Protein Eng.* 2, 577–582.
23. Hayes, J. J., and Wolffe, A. P. (1993) *Proc. Natl. Acad. Sci. U.S.A.* 15, 6415–6419.
24. Hayes, J. J., Pruss, D., and Wolffe, A. P. (1994) *Proc. Natl. Acad. Sci. U.S.A.* 91, 7817–7821.
25. Pruss, D., Bartholomew, B., Persinger, J., Hayes, J., Arents, G., Moudrianakis, E. N., and Wolffe, A. P. (1996) *Science* 274, 614–617.
26. Revel, H. R., and Luria, S. E. (1970) *Annu. Rev. Genet.* 4, 177–194.
27. Yen, S.-F., Germon, W., and Wilson, W. D. (1983) *J. Am. Chem. Soc.* 105, 3713–3719.
28. Synder, L., Gold, L., and Kutter, E. (1976) *Proc. Natl. Acad. Sci. U.S.A.* 73, 3098–3102.
29. Bradbury, E. M., Cary, P. D., Chapman, G. E., Crane-Robinson, C., Danby, S. E., Rattle, H. W., Boublik, M., Palau, J., and Aviles, F. J. (1975) *Eur. J. Biochem.* 52, 605–613.
30. Bradbury, E. M., Chapman, G. E., Danby, S. E., Hartman, P. G., and Riches, P. L. (1975) *Eur. J. Biochem.* 57, 521–528.
31. Tiktopulo, E. I., Privalov, P. L., Odintsova, T. I., Ermokhina, T. M., Krashennnikov, I. A., Aviles, F. X., Cary, P. D., and Crane-Robinson, C. (1982) *Eur. J. Biochem.* 122, 327–331.
32. Ramakrishnan, V., Finch, J. T., Graziano, V., Lee, P. L., and Sweet, R. M. (1993) *Nature* 362, 219–223.
33. Lennox, R. W., and Cohen, L. H. (1984) in *Histone Genes: Structure, Organization, and Regulation* (Stein, G. S., Stein, J. L., and Marzluff, W. F., Eds.) John Wiley & Sons, New York.
34. Wellman, S. E., Song, Y., Su, D., and Mamoon, N. M. (1997) *Biotechnol. Appl. Biochem.* 26, 117–123.
35. Aviles, F. J., Chapman, G. E., Kneale, G. G., Crane-Robinson, C., and Bradbury, E. M. (1978b) *Eur. J. Biochem.* 88, 363–371.
36. Chapman, G. E., Aviles, F. J., Crane-Robinson, C., and Bradbury, E. M. (1978) *Eur. J. Biochem.* 90, 287–296.
37. Scopes, R. K. (1987) *Protein Purification: Principles and Practice*, Springer-Verlag, New York.
38. Runnels, J., and Snyder, L. (1978) *Virology* 27, 815–818.
39. Sambrook, J., Fritsch, E. F., and Maniatis, T. (1989) *Molecular Cloning: A Laboratory Manual*, 2nd ed., Cold Spring Harbor Laboratory Press, Cold Spring Harbor, NY.
40. Hirschman, S. Z., and Felsenfeld, G. (1966) *J. Mol. Biol.* 16, 347–358.
41. Lu, Z. H., Sittman, D. B., Brown, D. T., Munshi, R., and Leno, G. H. (1997) *J. Cell Sci.* 110, 2745–2758.
42. Wellman, S. E., Song, Y., and Mamoon, N. M. (1999) *Biochemistry* 38, 13112–13118.
43. Spink, C. H., and Wellman, S. E. (2001) *Methods Enzymol.* 340, 193–211.
44. Bradbury, E. M., Danby, S. E., Rattle, H. W. E., and Giancotti, V. (1975) *Eur. J. Biochem.* 57, 97–105.
45. Pullman, B. (1983) *J. Biomol. Struct. Dyn.* 1, 773–794.
46. Jayaram, B., Sharp, K. A., and Honig, B. (1989) *Biopolymers* 28, 975–993.
47. Izaurralde, E., Käs, E., and Laemmli, U. K. (1989) *J. Mol. Biol.* 210, 573–585.
48. Käs, E., Izaurralde, E., and Laemmli, U. K. (1989) *J. Mol. Biol.* 210, 587–599.
49. Sevall, J. S. (1988) *Biochemistry* 27, 5038–5044.
50. Clark, D. J., Hill, C. S., Martin, S. R., and Thomas, J. O. (1988) *EMBO J.* 7, 69–75.
51. Kowalczykowski, S. C., Paul, L. S., Lonberg, N., Newport, J. W., McSwiggen, J. A., and von Hippel, P. H. (1986) *Biochemistry* 25, 1226–1240.

BI020199N